Science Bulletin 63 (2018) 282–286

Contents lists available at ScienceDirect

Science Bulletin

journal homepage: www.elsevier.com/locate/scib

Article

Experimental realization of honeycomb borophene

Wenbin Li [a,b], Longjuan Kong [a,b], Caiyun Chen [a,b], Jian Gou [a,b], Shaoxiang Sheng [a,b], Weifeng Zhang [c], Hui Li [d], Lan Chen [a,b,*], Peng Cheng [a,b,*], Kehui Wu [a,b,e,*]

[a] Institute of Physics, Chinese Academy of Sciences, Beijing 100190, China
[b] School of Physical Sciences, University of Chinese Academy of Sciences, Beijing 100049, China
[c] School of Physics and Electronics, Henan University, Kaifeng 475004, China
[d] Beijing Advanced Innovation Center for Soft Matter Science and Engineering, Beijing University of Chemical Technology, Beijing 100029, China
[e] Collaborative Innovation Center of Quantum Matter, Beijing 100871, China

ARTICLE INFO

Article history:
Received 20 January 2018
Received in revised form 1 February 2018
Accepted 2 February 2018
Available online 5 February 2018

Keywords:
Borophene
Honeycomb structure
2D materials

ABSTRACT

We report the successful preparation of a purely honeycomb, graphene-like borophene, by using an Al(1 1 1) surface as the substrate and molecular beam epitaxy (MBE) growth in ultrahigh vacuum. Scanning tunneling microscopy (STM) images reveal perfect monolayer borophene with planar, non-buckled honeycomb lattice similar as graphene. Theoretical calculations show that the honeycomb borophene on Al (1 1 1) is energetically stable. Remarkably, nearly one electron charge is transferred to each boron atom from the Al(1 1 1) substrate and stabilizes the honeycomb borophene structure, in contrast to the negligible charge transfer in case of borophene/Ag(1 1 1). The existence of honeycomb 2D allotrope is important to the basic understanding of boron chemistry, and it also provides an ideal platform for fabricating boron-based materials with intriguing electronic properties such as Dirac states.

1. Introduction

The boom of graphene research, as well as the successful development of high-quality graphene films for industrial applications [1,2], has inspired the theoretical prediction and experimental discovery of a number of elemental two-dimensional (2D) materials, such as silicene [3–5], germanene [6–8], stanene [9,10] and phosphorene [11]. Different from the planar honeycomb structure with sp^2 hybridization in graphene, these 2D materials tend to form buckled honeycomb lattice with mixed sp^2-sp^3 hybridization, due to their larger atomic radius as compared with carbon. An exceptional case is borophene, since boron possesses an even smaller atomic radius than carbon. However, as boron has only three valence electrons, the electron deficiency makes a honeycomb lattice of boron energetically unstable. Instead, a triangular lattice with periodic holes was predicted to be more stable [12–14]. Various stable structures of borophene sheets have been predicted, such as α, β and so on, with different arrangements of the holes in the triangular lattice [12,13,15–21]. And a few of them have been successfully synthesized on silver surface [22–26].

So far, all existing borophene lattices are a triangular lattice with periodic holes, or inversely, they can also be regarded as a honeycomb lattice with periodic boron adatoms. Therefore, a challenging question is that whether it is possible to prepare a borophene monolayer with a pure honeycomb lattice, or in other words, a graphene-like borophene. Honeycomb borophene is important due to two reasons. Firstly, a honeycomb lattice will naturally host Dirac fermions and thus intriguing electronic properties resembling other group IV elemental 2D materials [27]. Secondly, in the well-known high T_c superconductor, MgB_2, the crystal structure consists of boron planes with intercalated Mg layers, where the boron plane has a pure honeycomb structure like graphene [28]. It is remarkable that in MgB_2, superconductivity occurs in the boron planes, while the Mg atoms serves as electron donors [28]. Therefore, preparation of a honeycomb 2D boron lattice may open up opportunities in controlling the high T_c superconductivity by tuning the structure of boron-based compounds [29–31].

By employing molecular beam epitaxy (MBE) growth, we have successfully fabricated a 2D boron sheet with a purely honeycomb lattice by choosing an Al(1 1 1) surface as the substrate. The idea is that aluminum has three free electrons and thus can provide an effective compensation for the electron deficiency in borophene. Our scanning tunneling microscopy (STM) images reveal perfect monolayer borophene film with honeycomb lattice. In addition, theoretical calculations show that the honeycomb borophene on

* Corresponding authors.
E-mail addresses: lchen@iphy.ac.cn (L. Chen), pcheng@iphy.ac.cn (P. Cheng), khwu@iphy.ac.cn (K. Wu).

https://doi.org/10.1016/j.scib.2018.02.006
2095-9273/

Al(1 1 1) is energetically stable. Remarkably, nearly one electron charge is transferred to each boron atom from the Al(1 1 1) substrate, in contrast to the little charge transfer in B/Ag(1 1 1) case. This work demonstrates that the borophene lattice can be manipulated by controlling the charge transfer between the substrate and the borophene film [32,33]. The successful fabrication of honeycomb borophene provides attractive possibility to control superconductivity in boron-based compounds.

2. Methods

The experiments were performed both in a homebuilt low temperature-STM-MBE system (base pressure $\sim 1.0 \times 10^{-10}$ mbar) and a Unisoko USM 1300 system (base pressure $\sim 5.0 \times 10^{-11}$ mbar). Clean Al(1 1 1) substrate was prepared by cycles of Ar^+ ion sputtering and annealing. The borophene monolayers were prepared by evaporating pure boron (99.999%) on Al(1 1 1) using an e-beam evaporator, with the boron flux of about 0.1 monolayer per minute. The Al(1 1 1) substrate was held at a temperature about 500 K during growth. STM and scanning tunneling spectroscopy (STS) data were obtained either at 77 or 4.5 K. The STM data were processed by using the free WSxM software [34]. First principles calculations were performed within the framework of plane-wave density functional theory (DFT), as implemented in the Vienna *ab initio* Simulation Package (VASP) [35]. Generalized gradient approximation (GGA) with Perdew–Burke–Ernzerhof (PBE) function [36] was adopted to describe the exchange–correlation interaction. The interaction between valence and core electrons was described by the projector-augmented wave (PAW) [37]. For geometric optimization, both the lattice constants and positions of atoms were relaxed until the force on each atom was less than 0.001 eV/Å and the criterion for total energy convergence was 1.0×10^{-5} eV/atom. A kinetic energy cutoff of 400 eV was chosen for the plane-wave expansion. We applied periodic boundary conditions in all directions with a vacuum layer larger than 15 Å to avoid image-image interaction along the sheet thickness. The Brillouin zone was sampled by a $21 \times 21 \times 1$ Monkhorst-Pack *k*-mesh [38].

3. Results and discussion

Monolayer borophene islands are formed upon evaporation of boron onto clean Al(1 1 1) substrate at about 500 K, as shown in Fig. 1a and b. The measured height profile in Fig. 1c shows a single Al(1 1 1) step with height of 236 pm, as well as a height difference between monolayer borophene and the Al(1 1 1) substrate (320 pm). It is notable that the height of monolayer borophene exhibits little change with varying the scanning bias between (−6 V, +6 V) (as shown in Fig. 1d). With the increase of boron coverage, the borophene islands grow in size, and some of them can run cross the Al (1 1 1) substrate steps, as shown in Fig. 1b for example. The line profile in Fig. 1e reveals a single Al(1 1 1) step, with height of

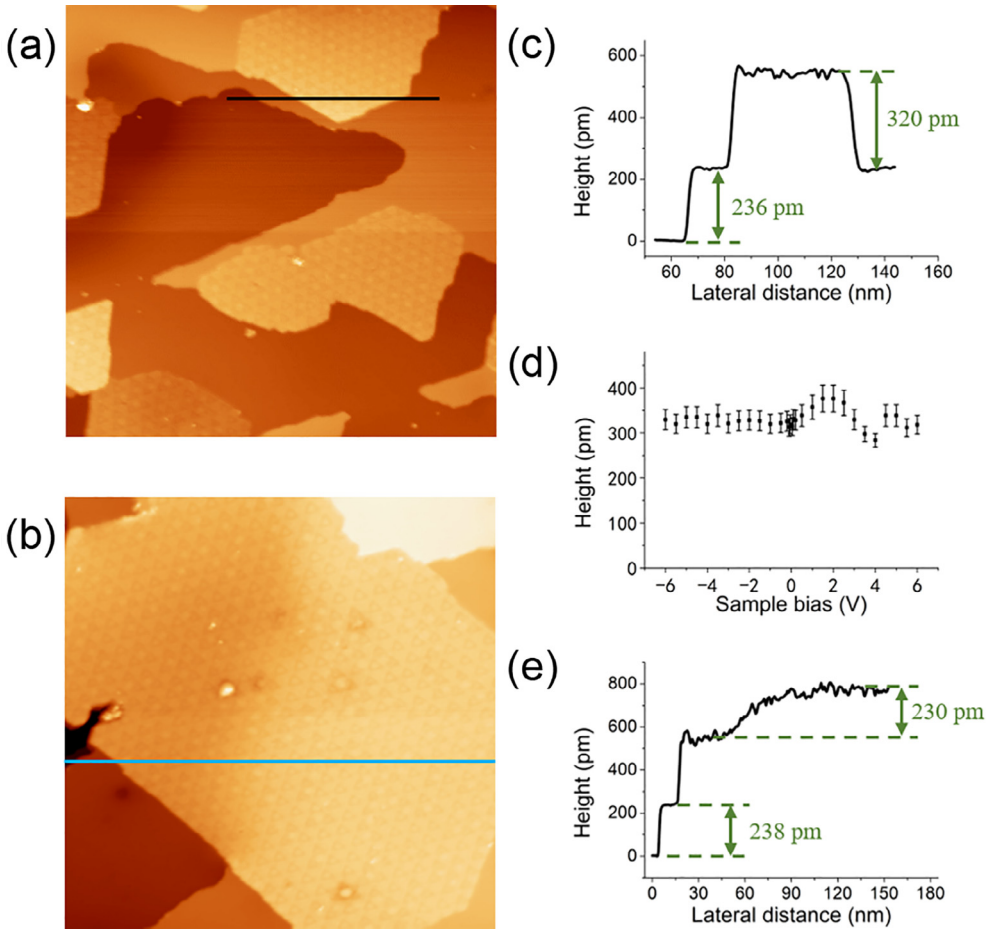

Fig. 1. (Color online) Monolayer borophene on Al(1 1 1). (a) STM image (180 nm × 180 nm) of borophene islands on Al(1 1 1) surface; (b) STM image (150 nm × 150 nm) showing a monolayer borophene island running across an Al(1 1 1) step. (c) Line profile along the black line in (a). (d) the measured height of single layer borophene at different bias voltages shows little change. (e) Line profile along the blue line in (b). The scanning parameters are: (a) sample bias −4.0 V, *I* = 50 pA; (b) sample bias −2.0 V, *I* = 50 pA.

230 pm, covered by the island without breaking the continuity of the borophene lattice.

High-resolution STM images reveal characteristic quasi-periodic, triangular corrugations on the surface of the borophene monolayer, as shown in Fig. 1 and the zoom-in image in Fig. 2a. The period of the corrugation is roughly 7 nm and height difference in the *z* directions are 40–60 pm. Such large corrugation patterns often occur due to strain relaxation on surfaces, such as the herringbone pattern on Au(1 1 1) surface [39,40], as will be discussed later. Importantly, atomically resolved STM images show a honeycomb lattice structure, as shown in Fig. 2b. The measured lattice constant is 0.29 nm, which is only a bit smaller than the calculated lattice constant of a free standing, honeycomb borophene (0.3 nm), and also close to the lattice constant of Al(1 1 1)−1 × 1 (0.286 nm). The honeycomb lattice is locally flat and without buckling, since the atoms in A and B sites of the honeycomb lattice appears equivalent in the STM images in Fig. 2b. On the other hand, the honeycomb lattice is overlapped on the large-periodic, triangular corrugation, as clearly illustrated in the 3D STM image in Fig. 2c, even though the atomic corrugation in the honeycomb lattice (∼1.5 pm) is much smaller than the triangular corrugation (40–60 pm). To conclude, our STM data show unambiguously that we have obtained honeycomb, graphene-like borophene monolayer on Al(1 1 1).

Previous theoretical works have already indicated that the honeycomb lattice is unstable for free-standing borophene [12]. Obviously, the Al(1 1 1) substrate plays a crucial role here in stabilizing the honeycomb borophene lattice. To understand the mechanism in detail, we performed first principles calculations and compared the stability of borophene on Al(1 1 1) and Ag(1 1 1), respectively. Honeycomb borophene 1 × 1 monolayer was overlapped with 1 × 1 unit cells of Al (1 1 1) and Ag (1 1 1) surfaces, respectively, as these two surfaces both have very small lattice mismatch with the honeycomb borophene 1 × 1. The substrates consist of 4 metal slabs with the bottom two slabs fixed, while the other two slabs and the borophene sheet fully relaxed in the geometric optimization. To estimate the stability of the honeycomb borophene sheet on different metal substrates, the formation energy is defined as:

$$E_f = (E_{tot} - E_{sub} - N \times E_B)/N,$$

where E_{tot} is the total energy of monolayer borophene on the metal substrate, E_{sub} is the total energy of the substrate, E_B is the energy per atom in the solid boron of α-B_{12} phase, and N is the number of boron atoms in each unit cell [41]. Under such definitions, a configuration with smaller E_f is more stable. After relaxation, the borophene lattice adopts a 1 × 1 lattice matching with the Al(1 1 1) substrate, with boron atoms located at the hollow site of the Al(1 1 1) lattice (Fig. 3a). The side view of the structure indicates that the borophene lattice is flat (as shown in Fig. 3b). Remarkably, there is a large amount of electron charge located at the interface [42] between the borophene monolayer and the Al(1 1 1) substrate, as revealed in the charge distribution map (Fig. 3c), suggesting a pronounced electron transfer from the first layer of the substrate to the borophene monolayer. The Bader charge analysis quantify that, in average, about 0.7 electron is transferred to each boron atom from the Al substrate. Similar theoretical calculations were also performed on Ag(1 1 1) surface (Fig. 3d–f). However, the formation energy of honeycomb borophene on Ag(1 1 1) is much bigger than that on Al(1 1 1), and also much bigger than other reported borophene structures (β_{12} and χ_3 phases). This is consistent with previous conclusions that the honeycomb borophene on Ag(1 1 1) is unstable. In addition, there is little electron accumulation at the interface, indicating negligible charge transfer between borophene and the Ag(1 1 1) substrate. The average formation energy and charge transfer of honeycomb borophene on Al(1 1 1) and Ag(1 1 1) substrates were list in Table 1.

It is not difficult to understand why Al(1 1 1) substrate can stabilize the honeycomb borophene lattice. Free-standing, honeycomb borophene lattice is unstable because of the electron deficiency of boron atoms. Thus, boron adatoms are required to fill in some honeycomb units to compensate for the electron deficiency [43]. On the other hand, if a boron atom can acquire one

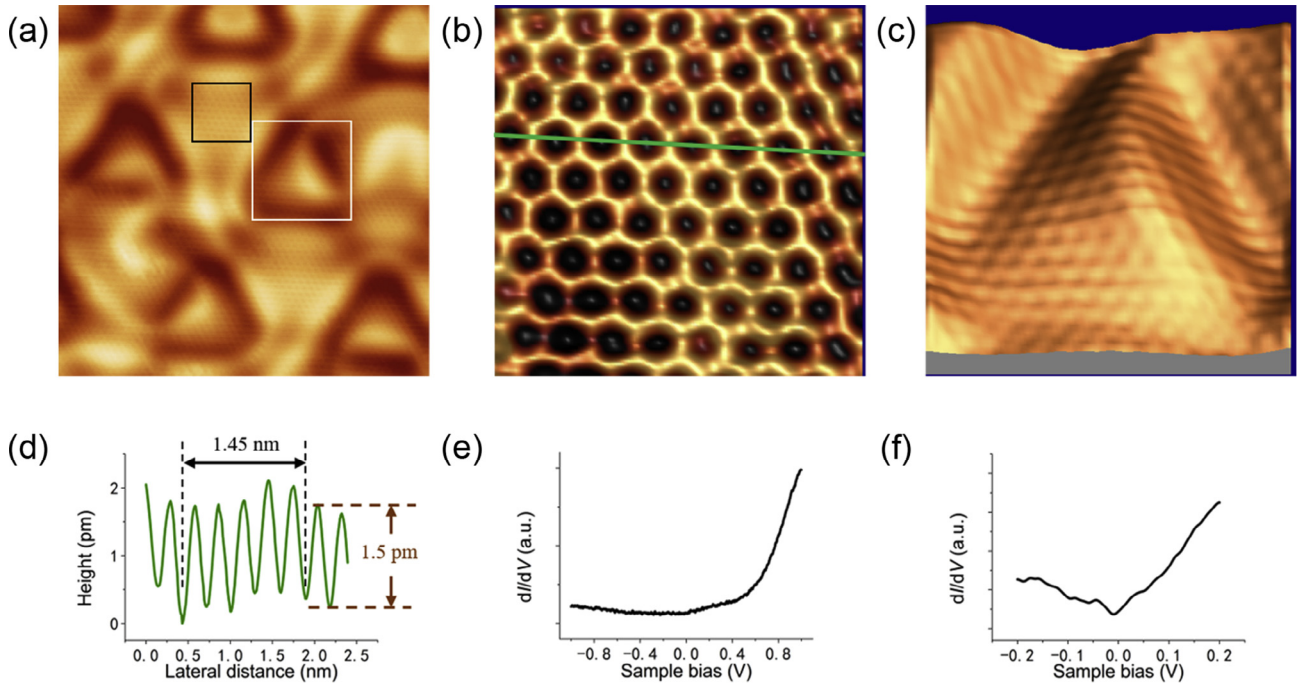

Fig. 2. (Color online) High resolution STM images and STS data on borophene monolayer on Al(1 1 1). (a) STM image (15 nm × 15 nm) showing the large-period, triangular corrugation. (b) A high resolution STM image (2.4 nm × 2.4 nm) of the area marked by black rectangle in (a), showing a flat honeycomb lattice. (c) 3D STM image (4 nm × 4 nm) of the area marked by white rectangle in (a). (d) line profile along green line in (b). (e, f) d*I*/d*V* curves taken on borophene surface with different bias voltage range. The scanning parameters for (a-c) are: sample bias −11 mV, *I* = 130 pA.

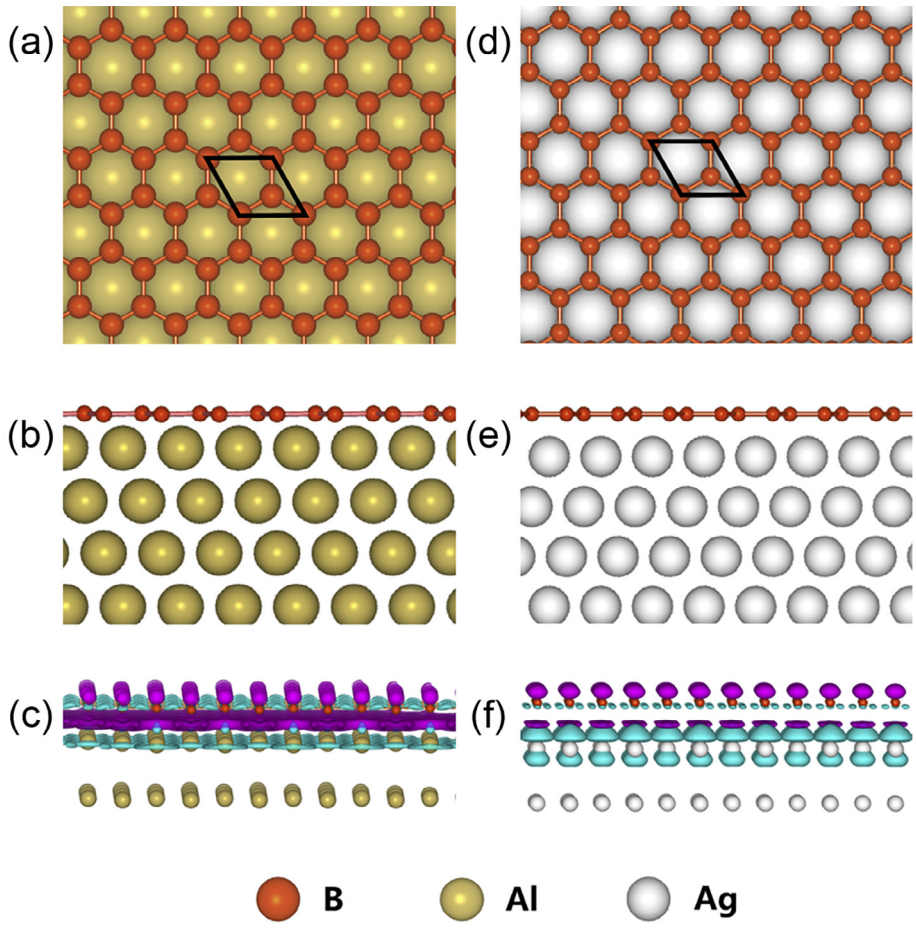

Fig. 3. (Color online) Structural models and electron density of honeycomb borophene on Al(1 1 1) and Ag(1 1 1). (a), (b) top and side views of honeycomb borophene on Al(1 1 1). (c) electron density map of honeycomb borophene on Al(1 1 1). (d), (e) top and side views of honeycomb borophene on Ag(1 1 1). (f) is the corresponding electron density map. In (c) and (f), the electron accumulation and depletion regions were presented by purple and cyan colors, respectively.

Table 1
Formation energy and averaged charge transfer in different structures of borophene. h-BS and β_{12}-BS represent honeycomb and β_{12} borophene structure, respectively.

	E_f (eV/atom)	Average charge per boron |e|
h-BS on Al (1 1 1)	0.31	−0.70
h-BS on Ag (1 1 1)	0.81	−0.06
β_{12}-BS on Ag(1 1 1)	0.35	−0.03

additional electron from the environment, the boron atom would become carbon-like, and the formation of a honeycomb lattice like graphene will be a natural choice. Aluminum is ideally substrate for this purpose considering its high electron density as well as small lattice mismatch with borophene. It can be imagined that if one chooses a series of metal surfaces with different free electron density and interaction with boron, it may be possible to synthesize various borophene structures with different hole density, for example between 1/6 (hole density of β_{12} on Ag(1 1 1)) and 1/3 (honeycomb borophene).

A graphene-like 2D lattice will intrinsically result in Dirac bands in its electronic structure. The honeycomb borophene monolayer on Al(1 1 1) should possess the same in-plane band structure as a free-standing, honeycomb borophene, with possibly a shift of Fermi level due to the electron transfer from the substrate [44]. The local electron states of honeycomb borophene were studied by STS as shown in Fig. 2e. The dI/dV curves indicate the honeycomb borophene is metallic. In particular, a V-shape dI/dV curve is revealed near the Fermi energy, with a dip at the Fermi energy (Fig. 2f), such feature is similar to characteristic of existence of the Dirac bands in graphene. A detail understanding on the origin of the V-shape dip, however, requires further studies, especially angle-resolved photoelectron spectroscopy (ARPES) measurements.

Finally, we discuss the mechanism for the formation of the quasi-periodic, triangular corrugation patterns. The amplitude of the triangular corrugation is about 40–60 pm and the distance between two triangles ranges from 6 to 7.5 nm. We noticed that the lattice constant of the honeycomb borophene lattice is varied slightly relative to the triangular corrugations. The periods are close to 0.29 nm in flat area, and close to 0.3 nm in corrugated area. Regarding the fact that borophene lattice is slightly compressed due to the interaction with the substrate, the appearance of such large period corrugation is very similar to the herringbone structure on Au(1 1 1) surface, where the relaxation of the compressed Au(1 1 1) lattice results in alternative hcp and fcc domains in a $22 \times \sqrt{3}$ superstructure. However, more detailed investigation on the triangular patterns requires heavy calculation task and is still in progress.

4. Conclusions

We have successfully synthesized graphene-like, flat honeycomb borophene monolayer on Al(1 1 1). Theoretical calculations found that the honeycomb borophene is stable on Al(1 1 1) surface, and there is nearly one electron transferred from the Al(1 1 1) substrate to each boron atom, which is the key for stabilizing the structure. Our work vividly demonstrated that one can manipulate the

borophene lattice by controlling the charge transfer [42] between the substrate and the borophene. And the honeycomb borophene provides attractive possibility to construct boron-based atomic layers with unique electronic properties such as Dirac states, as well as to control superconductivity in boron-based compounds.

Conflict of interest

The authors declare that they have no conflict of interest.

Acknowledgments

This work was supported by the National Key Research and Development Program (2016YFA0300904 and 2016YFA0202301), the National Natural Science Foundation of China (11334011, 11674366 and 11674368), and the Strategic Priority Research Program of the Chinese Academy of Sciences (XDB07010200 and XDPB06).

References

[1] Xu X, Yi D, Wang Z, et al. Greatly enhanced anticorrosion of Cu by commensurate graphene coating. Adv Mater 2017. https://doi.org/10.1002/adma.201702944.
[2] Xu X, Zhang Z, Dong J, et al. Ultrafast epitaxial growth of metre-sized single-crystal graphene on industrial Cu foil. Sci Bull 2017;62:1074–80.
[3] Zhao J, Liu H, Yu Z, et al. Rise of silicene: a competitive 2D material. Prog Mater Sci 2016;83:24–151.
[4] Feng B, Ding Z, Meng S, et al. Evidence of silicene in honeycomb structures of silicon on Ag(111). Nano Lett 2012;12:3507–11.
[5] Chen L, Liu C, Feng B, et al. Evidence for Dirac fermions in a honeycomb Lattice based on silicon. Phys Rev Lett 2012;109:056804.
[6] Li L, Lu SZ, Pan J, et al. Buckled germanene formation on Pt(111). Adv Mater 2014;26:4820–4.
[7] Derivaz M, Dentel D, Stephan R, et al. Continuous germanene layer on Al(111). Nano Lett 2015;15:2510–6.
[8] Gou J, Zhong Q, Sheng S, et al. Strained monolayer germanene with 1×1 lattice on Sb(111). 2D Mater 2016;3045005.
[9] Zhu FF, Chen WJ, Xu Y, et al. Epitaxial growth of two-dimensional stanene. Nat Mater 2015;14:1020–5.
[10] Gou J, Kong L, Li H, et al. Strain-induced band engineering in monolayer stanene on Sb(111). Phys Rev Mater 2017;1:054004.
[11] Zhang JL, Zhao S, Han C, et al. Epitaxial growth of single layer blue phosphorus: a new phase of two-dimensional phosphorus. Nano Lett 2016;16:4903–8.
[12] Tang H, Ismail-Beigi S. Novel precursors for boron nanotubes: the competition of two-center and three-center bonding in boron sheets. Phys Rev Lett 2007;99:115501.
[13] Yang X, Ding Y, Ni J. Ab initio prediction of stable boron sheets and boron nanotubes: structure, stability, and electronic properties. Phys Rev B 2008;77:041402(R).
[14] Tang H, Ismail-Beigi S. Self-doping in boron sheets from first principles: a route to structural design of metal boride nanostructures. Phy Rev B 2009;80:134113.
[15] Galeev TR, Chen Q, Guo JC, et al. Deciphering the mystery of hexagon holes in an all-boron graphene alpha-sheet. Phys Chem Chem Phys 2011;13:11575–8.
[16] Penev ES, Bhowmick S, Sadrzadeh A, et al. Polymorphism of two-dimensional boron. Nano Lett 2012;12:2441–5.
[17] Wu X, Dai J, Zhao Y, et al. Two-dimensional boron monolayer sheets. Acs Nano 2012;6:7443–53.
[18] Liu Y, Penev ES, Yakobson BI. Probing the synthesis of two-dimensional boron by first-principles computations. Angew Chem Int Ed 2013;52:3156–9.
[19] Piazza ZA, Hu HS, Li WL, et al. Planar hexagonal B(36) as a potential basis for extended single-atom layer boron sheets. Nat Commun 2014;5:3113.
[20] Li WL, Chen Q, Tian WJ, et al. The B35 cluster with a double-hexagonal vacancy: a new and more flexible structural motif for borophene. J Am Chem Soc 2014;136:12257–60.
[21] Wang LS. Photoelectron spectroscopy of size-selected boron clusters: from planar structures to borophenes and borospherenes. Int Rev Phys Chem 2016;35:69–142.
[22] Feng B, Zhang J, Zhong Q, et al. Experimental realization of two-dimensional boron sheets. Nat Chem 2016;8:563–8.
[23] Mannix AJ, Zhou XF, Kiraly B, et al. Synthesis of borophenes: anisotropic, two-dimensional boron polymorphs. Science 2015;350:1513–6.
[24] Zhang ZH, Mannix AJ, Hu ZL, et al. Substrate-induced nanoscale undulations of borophene on silver. Nano Lett 2016;16:6622–7.
[25] Zhong Q, Kong L, Gou J, et al. Synthesis of borophene nanoribbons on Ag(110) surface. Phys Rev Mater 2017;1:021001(R).
[26] Zhong Q, Zhang J, Cheng P, et al. Metastable phases of 2D boron sheets on Ag(1 1 1). J Phys Condens Matter 2017;29:095002.
[27] Liu CC, Jiang H, Yao Y. Low-energy effective Hamiltonian involving spin-orbit coupling in silicene and two-dimensional germanium and tin. Phys Rev B 2011;84:195430.
[28] Buzea C, Yamashita T. Review of the superconducting properties of MgB_2. Supercond Sci Tech 2001;14:R115–46.
[29] Penev ES, Kutana A, Yakobson BI. Can two-dimensional boron superconduct? Nano Lett 2016;16:2522–6.
[30] Gao M, Li QZ, Yan XW, et al. Prediction of phonon-mediated superconductivity in borophene. Phys Rev B 2017;95:024505.
[31] Cheng C, Sun JT, Liu H, et al. Suppressed superconductivity in substrate-supported β_{12} borophene by tensile strain and electron doping. 2D Mater 2017;4:025032.
[32] Zhang Z, Yang Y, Gao G, et al. Two-dimensional boron monolayers mediated by metal substrates. Angew Chem Int Ed 2015;54:13022–6.
[33] Zhang Z, Penev ES, Yakobson BI. Two-dimensional materials: polyphony in B flat. Nat Chem 2016;8:525–7.
[34] Horcas I, Fernandez R, Gomez-Rodriguez JM, et al. WSXM: a software for scanning probe microscopy and a tool for nanotechnology. Rev Sci Instrum 2007;78:013705.
[35] Kresse G, Furthmuller J. Efficient iterative schemes for ab initio total-energy calculations using a plane-wave basis set. Phys Rev B 1996;54:11169–86.
[36] Perdew JP, Burke K, Ernzerhof M. Generalized gradient approximation made simple. Phys Rev Lett 1996;77:3865–8.
[37] Kresse G, Joubert D. From ultrasoft pseudopotentials to the projector augmented-wave method. Phys Rev B 1999;59:1758–75.
[38] Monkhorst HJ, Pack JD. Special points for brillouin-zone integrations. Phys Rev B 1976;13:5188–92.
[39] Barth JV, Brune H, Ertl G, et al. Scanning tunneling microscopy observations on the reconstructed Au(111) surface-atomic-struture, long-rang superstructure, rotational domains, and surface-defects. Phys Rev B 1990;42:9307–18.
[40] Hanke F, Bjork J. Structure and local reactivity of the Au(111) surface reconstruction. Phys Rev B 2013;87:235422.
[41] Donohue J. Structures of the elements. John Wiley & Sons Inc; 1974.
[42] Zhang Z, Shirodkar SN, Yang Y, et al. Gate-voltage control of borophene structure formation. Angew Chem Int Ed 2017;56:15421–6.
[43] Evans MH, Joannopoulos JD, Pantelides ST. Electronic and mechanical properties of planar and tubular boron structures. Phys Rev B 2005;72:045434.
[44] Zhang LZ, Yan QB, Du SX, et al. Boron sheet adsorbed on metal surfaces: structures and electronic properties. J Phys Chem C 2012;116:18202–6.